

One-Pot Synthesis of Highly Luminescent CdSe/CdS Core–Shell Nanocrystals via Organometallic and “Greener” Chemical Approaches[†]

Ivo Mekis, Dmitri V. Talapin,* Andreas Kornowski, Markus Haase, and Horst Weller*

Institute of Physical Chemistry, University of Hamburg, Bundesstrasse 45, 20146 Hamburg, Germany

Received: December 27, 2002; In Final Form: April 9, 2003

We report different approaches to the synthesis of size series of highly luminescent CdSe/CdS core–shell nanocrystals. The mixture of hexadecylamine (HDA)–trioctylphosphine oxide (TOPO)–trioctylphosphine (TOP) as stabilizing solvent was found to be very suitable for one-pot synthesis of nearly monodisperse CdSe nanocrystals followed by growing the CdS shell of a desired thickness. The obtained CdSe/CdS nanocrystals exhibited a narrow PL band (fwhm \sim 27–35 nm) with reproducible room-temperature quantum yields as high as 50–85%. The emission color is tunable from green to red with increasing diameter of CdSe cores and/or thickness of the CdS shell. The possibility of preparing high-quality CdSe/CdS core–shell nanocrystals from the precursors cadmium acetate and H₂S, which are more environmentally benign than conventional ones (e.g., dimethylcadmium) used in the organometallic synthesis of nanocrystals, was demonstrated. General aspects of the nanocrystal nucleation and growth as well as applicability of “greener” synthetic schemes for synthesis of core–shell nanocrystals are discussed.

Introduction

Semiconductor nanocrystals synthesized by means of colloidal chemistry techniques provide a successful realization of the strong quantum confinement regime¹ with an advantage of continuous tunability of the electronic and optical properties by changing the physical size of the nanocrystals.^{2,3} Due to the excellent luminescent properties and relatively low cost in combination with the high chemical flexibility (e.g., colloidal nanocrystals can be handled in solution like ordinary molecular chemical substances), semiconductor nanocrystals are currently being investigated as emitting materials for thin-film light-emitting devices (LEDs),^{4,5} low-threshold lasers,⁶ optical amplifier media for telecommunication networks,⁷ and biological labels.^{8,9} A new field of research has recently emerged on the use of individual monodisperse nanocrystals as building blocks for the fabrication of quantum dot superstructures and the investigation of the collective properties of these novel artificial solids.^{10,11}

In recent years, tremendous advances in colloid chemistry led to the preparation of high-quality nanocrystals for several II–VI^{12–16} and III–V^{17–20} semiconductors. However, CdSe nanocrystals still remain the most extensively investigated among semiconductor nanoparticles, probably because of very successful preparation methods allowing an outstanding degree of control over the nanocrystal size, shape, and monodispersity.^{13,16,21} Thus, the synthesis of CdSe nanocrystals from dimethylcadmium and tri-*n*-octylphosphine selenide (TOPSe) at 250–300 °C in tri-*n*-octylphosphine oxide (TOPO)–tri-*n*-octylphosphine (TOP) mixture yields highly crystalline CdSe nanocrystals with sizes tunable from \sim 1.7 to 15 nm.¹² Introducing hexadecylamine (HDA) as a cosurfactant to the TOPO–TOP stabilizing mixture narrows the size distribution of CdSe

nanocrystals during their growth and allows a considerable improvement of their photoluminescence (PL) properties.¹³ Recently, novel “greener” synthetic schemes²² using environmentally more benign cadmium precursors (cadmium oxide,^{23–26} cadmium carbonate,²⁶ and cadmium acetate^{26,27}) were proposed as an alternative to the classical organometallic route¹² based on highly toxic, expensive, and pyrophoric Cd(CH₃)₂. A potential interest in these new cadmium precursors is caused by the so-called “green chemical principles” and is motivated by the development of “user-friendly” chemical methodologies and materials.²² Moreover, it has been shown that the “greener” recipes combined with the HDA–TOPO–TOP approach¹³ can lead to CdSe nanocrystals with room-temperature photoluminescence quantum efficiency (PL QE) up to 85%.²³

A large step toward the preparation of durable highly luminescent nanocrystals was the passivation of their surface with an inorganic shell of a semiconductor with wider band gap in analogy with the well-developed techniques for the growth of 2D quantum wells. Various II–VI semiconductors were investigated as shell material for CdSe nanocrystals. Thus, ZnS,^{13,28,29} CdS,³⁰ or ZnSe³¹ shells grown around CdSe core results in drastic improvement of PL efficiency and, especially, the chemical stability and photostability of the nanocrystal properties. The ZnS shell potentially provides a better stability compared to the CdS or ZnSe shells. However, the intrinsic strains coming from relatively large lattice mismatch between CdSe and ZnS (\sim 12%) result in defects within the ZnS shell if the shell thickness exceeds ca. 1.5 monolayers.²⁹ Moreover, the PL QE of CdSe/ZnS nanocrystals decreases with increasing core size, and the reported values for red-emitting CdSe/ZnS nanocrystals are relatively low (10–40%).^{29,32–34} The lattice mismatch between CdSe and CdS is considerably lower (\sim 3.9%).³⁰ This facilitates an epitaxial growth of a CdS shell around CdSe cores and, as a consequence, permits higher PL QE values to be achieved.³⁰ Moreover, CdSe/CdS nanocrystals have potential advantages for optoelectronic applications (e.g., LEDs) due to better electronic accessibility of CdSe emitting core.^{30,35}

[†] Part of the special issue “Arnim Henglein Festschrift”.

* To whom correspondence should be addressed. E-mail addresses: talapin@chemie.uni-hamburg.de (D. V. Talapin), weller@chemie.uni-hamburg.de (H. Weller). Fax: +49-40-42838-3452. Homepage: <http://www.chemie.uni-hamburg.de/pc/AKS/Weller/>.

The possibility to perform a synthesis of core-shell nanocrystals in one vessel has great advantages compared to a two-step preparation with different crude solutions for core and shell growth. The one-pot approach can be realized only if both core and shell can grow controllably in the same reaction mixture. Moreover, narrow size distributions of as-prepared cores are strongly desirable. There are one-pot synthetic routes for CdSe/ZnS²⁸ and CdSe/ZnSe³¹ nanocrystals, whereas the attempts of one-pot preparation of luminescent CdSe/CdS core-shells were unsuccessful.³⁰

In this paper we present easy and versatile one-pot synthetic routes for CdSe/CdS core-shell nanocrystals. The HDA-TOPO-TOP stabilizing mixture allows perfect control over both the core size and the shell thickness, keeping the particle size distribution below 10% at all stages of the preparation. We also compare "greener" versus organometallic approaches and discuss general advantages and disadvantages of both methods for the synthesis of core-shell nanocrystals.

Experimental Section

Chemicals. All chemicals used were of analytical grade or of highest purity available. Toluene, methanol, *n*-hexane (all anhydrous, Aldrich), cadmium acetate (Cd(Ac)₂, 99.99%, ChemPur), selenium (99.999%, ChemPur), bis(trimethylsilyl)sulfide (Aldrich), *n*-octylphosphonic acid (OPA, 99%, Alfa Aesar), *n*-tetradecylphosphonic acid (TDPA, 99%, Alfa Aesar), and H₂S gas (1-L bottles, Messer Griesheim) were used as received. Dimethylcadmium (99.99%, EpiChem) was filtered through a 0.2- μ m PTFE filter and stored at -35 °C in a glovebox. Tri-*n*-octylphosphine (further referred to as TOP, 90%, Fluka) was purified by distillation. Tri-*n*-octylphosphine oxide (TOPO, >98%, Merck, or >90%, Alfa Aesar) and hexadecylamine (HDA, >92%, Merck) were dried and degassed in the reaction vessel by heating under vacuum for 1 h at temperatures slightly below their boiling points.

Apparatus. UV-vis absorption spectra were measured at room temperature with a Cary 50 UV-vis spectrometer (Varian). Photoluminescence (PL) spectra were measured at room temperature with a FluoroMax-2 spectrofluorimeter (Instruments SA) on colloidal solutions having an optical density of less than 0.2 at the excitation wavelength (400 or 450 nm). Powder XRD measurements were performed on a Philips X'Pert PRO X-ray diffraction system. Samples for XRD measurements were prepared by dropping a colloidal suspension of nanocrystals in chloroform or hexane on a standard single-crystal Si support and evaporating the solvent. High-resolution transmission electron microscopy (HRTEM) and energy-dispersive X-ray analysis (EDAX) were performed on a Philips CM-300 microscope operating at 300 kV. Samples for TEM investigations were prepared by dropping dilute solutions of properly washed nanocrystals in toluene or chloroform onto 400-mesh carbon-coated copper grids, allowing the solvent to immediately evaporate.

PL Quantum Efficiency Measurements. All PL spectra of colloidal solutions were measured at optical densities at the excitation wavelength below 0.10. The small values of optical density guaranty that no artifacts can arise from different light penetration depths and reabsorption of emitted light. The photoluminescence excitation spectra were found to be nearly identical to the absorption spectra in a wide spectral region for all samples studied. The latter indicates no dependence of the emission spectra on the excitation wavelength, which is a good hint for the homogeneity of the sample. The absolute values of

room-temperature PL efficiency were determined by comparison of the PL intensity of a nanocrystal sample with that of the solution of Rhodamin 6G (laser grade, Lambda Physik) in absolute ethanol. We measured the absorption spectra of both the dye and the nanocrystal sample and used the wavelength spectra as the excitation wavelength for recording the emission spectra. This simple trick allowed the PL spectra corresponding to exactly equal optical density of the dye and the nanocrystals to be obtained. The PL intensity was integrated vs photon energy over the entire emission spectrum, and the literature value of 0.95 was taken for the room-temperature PL efficiency of Rodamine 6G in ethanol.³⁶ No correction of the PL QE value for the difference in refractive index of the solvents was performed. The error is, however, smaller than 5% for the solvents used. The measurement error of the PL quantum yield was estimated to be about 10%.

"Greener" Synthesis of CdSe Nanocrystals in a HDA-TOPO-TOP-TDPA Mixture. All "greener" synthetic routes were carried out under nitrogen using Schlenk technique. All substances were dried and degassed before use in order to provide rigorously oxygen- and water-free conditions for the synthesis. In a typical recipe, 8 g of TOPO were dried and degassed under vacuum at 180 °C for ca. 1 h in a 50-mL three-neck flask. Then, TOPO was cooled to 80–120 °C, 5 g HDA and 0.15 g TDPA were added, and the drying process was continued at 120 °C under vacuum for 20 min. The stock solution of TOPSe prepared by dissolving selenium (0.158 g, 2.0 mmol) in 2 mL of TOP was added and the mixture was heated to 300 °C. The cadmium stock solution (0.12 g of Cd(Ac)₂ in 3 mL of TOP) was quickly injected under vigorous stirring, resulting in nucleation of CdSe nanocrystals. Further particle growth was carried out at 260 °C. Both cadmium and selenium stock solutions were prepared and stored inside a glovebox under nitrogen atmosphere.

Organometallic Synthesis of CdSe Core Nanocrystals in a HDA-TOPO-TOP Mixture. CdSe nanocrystals were also synthesized in HDA-TOPO-TOP mixtures as described in ref 13, using dimethylcadmium and TOPSe as cadmium and selenium precursors, correspondingly. The molar ratio between cadmium and selenium precursors was 1.4:1. The injection of the stock solution (dimethylcadmium and TOPSe dissolved in TOP), as well as the further nanocrystal growth, was carried out at 300 °C. Addition of 1 wt % of octylphosphonic acid to TOPO allowed us to achieve more narrow particle size distributions and an improved reproducibility of nanocrystal growth rates.

The growth of CdSe nanocrystals was monitored by taking aliquots from the reaction mixture and measuring their UV-vis spectra. The reaction was stopped by cooling the reaction flask when the desired particle size was achieved. The duration of particle growth ranged from minutes to hours. As-prepared CdSe nanocrystals have relatively narrow size distributions and, therefore, no post-preparative size selection was necessary.

Synthesis of CdSe/CdS Core/Shell Nanocrystals by Injecting H₂S Gas. A CdS shell was grown around CdSe nanocrystals via a simple procedure. The reaction flask containing a freshly prepared crude solution of CdSe nanocrystals was heated to 140 °C. A certain amount of H₂S gas was slowly injected in 2-mL portions (~1 injection per 10–15 min) through a septum, using a Hamilton syringe. Note that the H₂S gas was injected *above* the solution not bubbled through the reaction mixture (the nitrogen flow within the Schlenk line was stopped before the injection). The reaction mixture slowly absorbed the H₂S gas

during stirring at 140 °C for half an hour. Then the temperature was decreased to 100 °C and the solution was stirred for one more hour. The reaction mixture was cooled to ~50 °C, and 15 mL of chloroform were added in order to prevent solidification of TOPO and HDA upon cooling to room temperature. In some cases the reaction mixture was slightly turbid after cooling to the room temperature, containing a white solid (presumably unreacted cadmium acetate). In this case the nanocrystal solution was filtrated through a PTFE 0.2- μ m syringe filter. Highly luminescent CdSe/CdS nanocrystals were isolated from the crude solution by precipitating them with methanol. The mixture was filtrated or centrifuged and the precipitate was redissolved in chloroform or toluene.

The volume of injected H₂S gas was dependent on the size of the CdSe cores. Thus, for the amount CdSe nanocrystals described in the typical synthesis we injected the following volumes of H₂S gas. For CdSe nanocrystals with sizes from ~2.5 to 3.5 nm the best core-shell particles were obtained by injecting 8–10 mL of H₂S (in portions of 2 mL), for a crude solutions of ~4 nm CdSe nanocrystals we used 6–8 mL of H₂S, and for nanocrystals larger than ~5 nm we injected 4–6 mL of H₂S.

In variation to the recipe described, the CdS shell can also be grown around CdSe the nanocrystals prepared from dimethylcadmium and TOPSe. In this case the addition of cadmium acetate is necessary before injecting H₂S. The amount of added cadmium acetate determines the thickness of the CdS shell formed. Typically, 3 mL of the crude solution of organometallically synthesized CdSe nanocrystals (~30 mg of CdSe) were mixed with 4 g of TOPO (Merck, 98%), 2 g of HDA, and 0.06 g of cadmium acetate. Then, 3 mL of H₂S were injected at 140 °C as described above. The reaction mixture was allowed to stir at 140 °C for half an hour, thereby absorbing the H₂S gas. Finally, the temperature was decreased to 100 °C and the solution was stirred for one more hour.

Synthesis CdSe/CdS Nanocrystals from Organometallic Shell Precursors. The CdSe/CdS core-shell nanocrystals with a tunable size of the CdSe cores and a desired thickness of CdS shell can also be synthesized in a HDA-TOPO-TOP mixture using organometallic precursors. Usually this synthesis was performed inside a nitrogen-filled glovebox. A typical preparation is the following: first, nearly monodisperse ~3.4-nm CdSe nanocrystals were synthesized from dimethylcadmium and TOPSe in the HDA-TOPO-TOP mixture as described above. Then, 3.6 mL of the crude solution of CdSe nanocrystals containing ~32 mg of CdSe were mixed with 7.5 g of TOPO and 5 g of HDA, the reaction mixture was heated to 140 °C, and the desired amount of Cd:S stock solution was added dropwise (~1 drop/s). The stock solution for growing CdS shell was prepared by mixing 0.05 mL of dimethylcadmium, 0.20 mL of bis(trimethylsilyl)sulfide, and 5 mL of TOP. The amount of the stock solution necessary to obtain a CdS shell with a desired thickness can be calculated from the ratio between the core and shell volumes by using the bulk lattice parameters of CdSe and CdS. After addition of the stock solution, the reaction mixture was cooled to 90 °C and was left for 1 h under stirring. Finally, the solution was cooled to room temperature and highly luminescent CdSe/CdS nanocrystals were isolated by filtration or centrifugation after precipitating them with methanol. A similar procedure was used for preparation of nanocrystals with different sizes of CdSe core. The obtained nanocrystals were soluble in various organic solvents such as chloroform, hexane, toluene, etc.

Comparison of the Stability of the PL Properties of CdSe, CdSe/CdS, and CdSe/ZnS Nanocrystals under UV Illumination. Highly luminescent CdSe nanocrystals (initial PL QE ~52%) were prepared in the HDA-TOPO-TOP mixture by the method of Peng et al.²³ from cadmium stearate and TOPSe. CdSe/ZnS core-shells were synthesized also in the HDA-TOPO-TOP mixture as described in ref 13. The nanocrystals with similar peak emission wavelengths (595–610 nm) were isolated from the crude solutions, redissolved in air-saturated chloroform, and placed in standard 1-cm quartz cells. Note that the amount of organic ligands washed out during the isolation of the particles from the crude solution can vary from sample to sample. Therefore, to diminish the impact of the sample pretreatment, we added to each cell 100 μ L of a solution containing 0.1 g of TOPO, 0.1 g of HDA, and 0.2 mL of TOP dissolved in 2 mL of chloroform. The optical density of each sample at the irradiation wavelength (366 nm) was adjusted to 0.1 ± 0.02 . Then, all cells were simultaneously illuminated by a lamp with 8-W output power at 366 nm. Special attention has been paid in order to achieve identical light intensities incident on each sample. The UV-Vis and PL spectra were recorded for each sample in certain time intervals and the temporal evolution of the nanocrystal PL QE was calculated from the spectra.

Results and Discussion

Synthesis of CdSe Nanocrystals from Cadmium Acetate and Dimethylcadmium in HDA-TOPO-TOP Mixture. The synthesis of CdSe nanocrystals from cadmium acetate (further referred to as Cd(Ac)₂) and TOPSe allows preparation of CdSe nanocrystals with narrow size distribution in a broad range of nanocrystal sizes. The use of an excess the selenium precursor is important for controllable growth and a narrow particle size distribution.^{23,38} Addition of tetradecylphosphonic acid (TDPA) to the HDA-TOPO-TOP stabilizing mixture results in slowing nanocrystal growth, i.e., a condition which is favorable for good crystallinity. Addition of TDPA also improves the size distribution, especially at late stages of particle growth. TDPA, probably, plays the role of a cosurfactant, binding to the particle surface and thus slowing the overall growth rate.²⁵ Moreover, the relatively stable complex of cadmium with TDPA can play the role of the monomer during the Ostwald ripening at a late stage of particle growth when all free Cd(Ac)₂ is consumed.

Nanocrystal growth was monitored by the shift of the absorption edge and the PL maximum toward longer wavelengths with increasing nanocrystal size. The left part of Figure 1 shows the evolution of the absorption spectrum of the reaction mixture during the growth of CdSe nanoparticles at 260 °C. After injection of Cd(Ac)₂ stock solution at 300 °C, the nanocrystals nucleate and grow at 260 °C up to ~5 nm during the first hour of heating. The reaction can be quenched at any stage by cooling the reaction mixture, thus allowing the preparation of nanocrystals of a desired size. The powder diffraction pattern corresponds to the hexagonal wurtzite CdSe phase and reveals a high degree of crystallinity of the nanocrystals. TEM and HRTEM investigations show that the CdSe nanocrystals usually exhibit a nearly spherical shape and narrow size distribution with a standard deviation below 10% (see Figure 5).

The CdSe nanocrystals synthesized from Cd(Ac)₂ exhibited solely band edge photoluminescence with nearly symmetric and narrow (fwhm ~25–35 nm) PL band shifting from bluish-green to red with increasing particle size. The room-temperature quantum yield of as-prepared CdSe nanocrystals usually is of 10–30%. However, it was observed that in some cases the PL

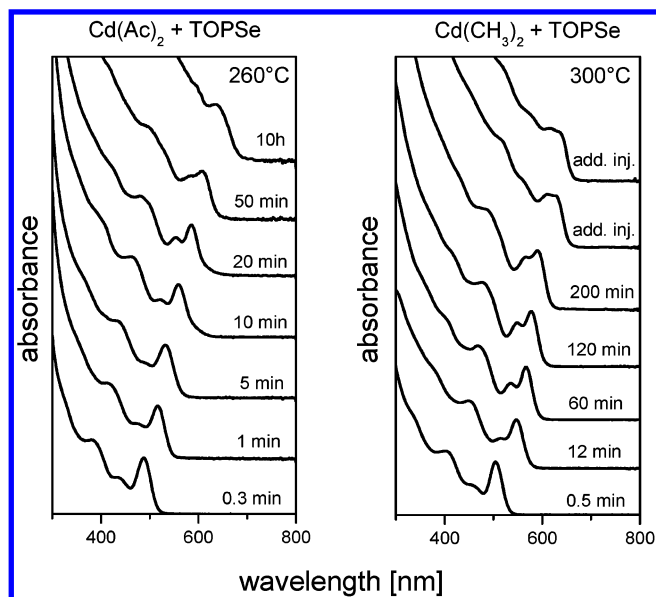


Figure 1. Temporal evolution of the absorption spectra of crude solutions during the synthesis of CdSe nanocrystals from (left) cadmium acetate and TOPSe at 260 °C and (right) from dimethylcadmium and TOPSe at 300 °C.

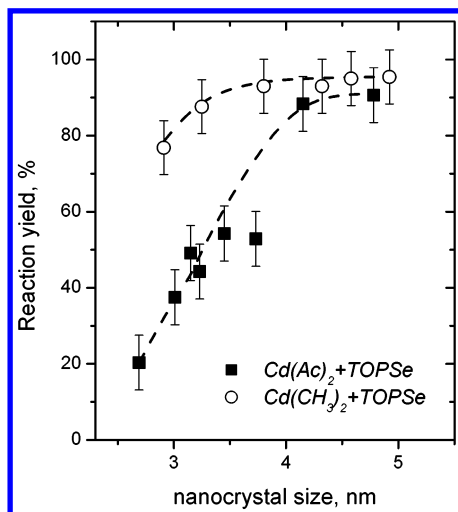


Figure 2. Evolution of the reaction yield during synthesis of CdSe nanocrystals from (■) cadmium acetate and TOPSe at 260 °C and (○) from dimethylcadmium and TOPSe at 300 °C. The data show that in the former case nanocrystals grow in the “focusing” regime and in the latter case via nano-Ostwald ripening.

QE of CdSe nanocrystals prepared from $\text{Cd}(\text{Ac})_2$ slowly improved upon storage of the crude solutions diluted with toluene at room temperature. Some samples after ~ 3 weeks of storage exhibited PL QE as high as $\sim 55\%$. Oxidation of the nanocrystal surface could not be responsible for the PL improvement, because similar behavior was observed for samples stored both in air and inside a nitrogen-purged glovebox. Probably, a slow surface reconstruction of as-prepared CdSe takes place at room temperature, resulting in better electronic passivation of surface dangling bonds with capping ligands.

To further investigate the processes during the synthesis of CdSe nanocrystals, we compared the preparations from $\text{Cd}(\text{Ac})_2$ and $\text{Cd}(\text{CH}_3)_2$. In the $\text{Cd}(\text{Ac})_2$ preparation in the HDA–TOPO–TOP mixture the nanoparticles grow considerably faster than those formed from $\text{Cd}(\text{CH}_3)_2$. The difference in growth rates exceeds an order of magnitude if the reaction is performed at the same temperature (e.g., 280 °C). Typically, we used the

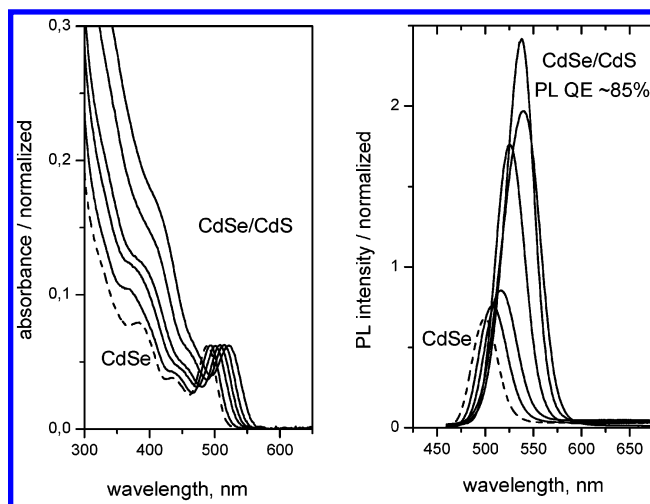


Figure 3. Effect of H_2S gas injection at 140 °C into the crude solution of CdSe nanocrystals prepared from $\text{Cd}(\text{Ac})_2$ and TOPSe. The UV–vis and PL spectra of initial solution of CdSe cores are shown with dashed curves. Progressive addition of H_2S gas (2, 4, 6, 8, 10 mL) resulted in red shifts of both UV–vis and PL spectra (solid lines, from left to right).

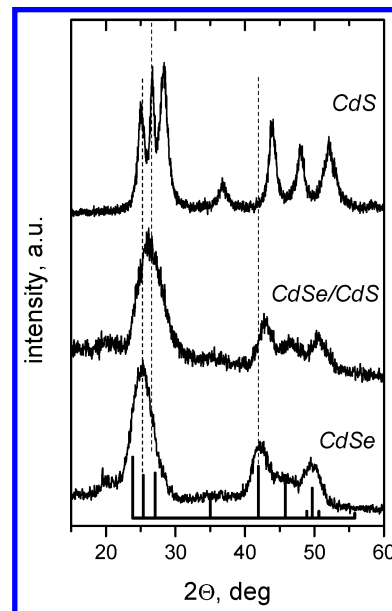


Figure 4. Wide-angle powder X-ray diffractograms of CdSe nanocrystals before and after injecting H_2S gas. The XRD pattern of CdS nanocrystals synthesized in the HDA–TOPO–TOP mixture is added for comparison.

growth temperature of 260 °C for cadmium acetate as precursor because this temperature was found to be optimal for a narrow particle size distribution. The growth of CdSe nanocrystals from dimethylcadmium at 260 °C is too slow, and we used a reaction temperature of 300 °C to accelerate the growth (Figure 1).

We also estimated and compared for both synthetic schemes the degree of conversion of precursors into CdSe nanocrystals (further referred to as “reaction yield”) at different stages of synthesis. Note, that in case of the synthesis from $\text{Cd}(\text{Ac})_2$ we used a large excess of TOPSe, whereas the synthesis from $\text{Cd}(\text{CH}_3)_2$ was performed with an excess of Cd precursor (initial Cd:Se ratio was $\sim 1.4:1$). The reaction yields were calculated with respect to the deficient component by taking aliquots from the reaction mixture, measuring the absorption spectra after cooling, and diluting with chloroform. The mean particle size and the molar concentration of CdSe nanocrystals were calculated using the published sizing curve^{38,39} and the size-dependent

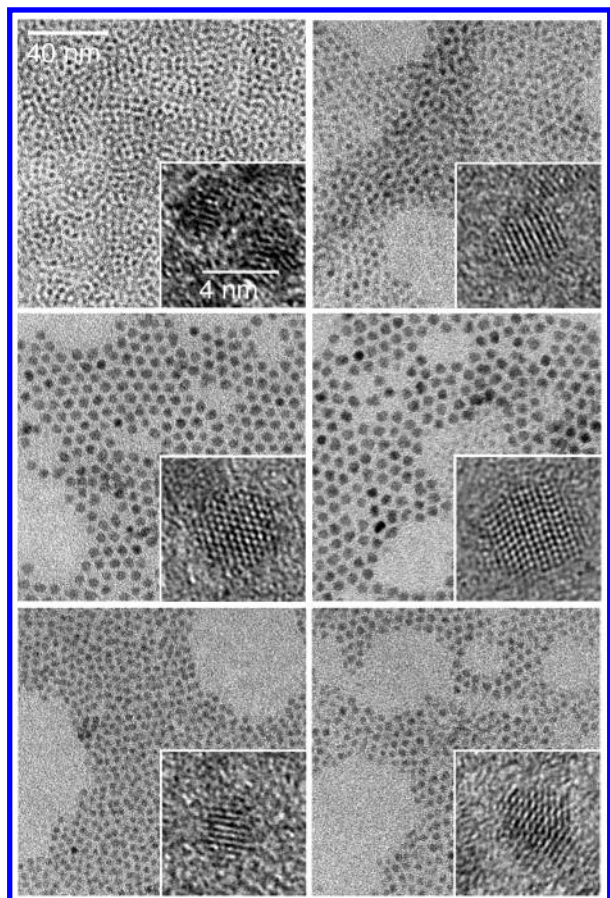


Figure 5. Overview TEM and HRTEM images of CdSe nanocrystals (left) and CdSe/CdS core–shells prepared from these cores (right). The core–shell particles were synthesized either by injecting H_2S gas into crude solutions of ~ 3.0 nm (top) and ~ 4.8 nm (middle) CdSe nanocrystals prepared from $\text{Cd}(\text{Ac})_2$ and TOPSe or by adding dimethylcadmium and bistrimethylsilylsulfide into a crude solution of CdSe nanocrystals prepared from organometallic precursors (bottom).

molar extinction coefficient at the first absorption maximum.³⁹ Some crude solutions of CdSe nanocrystals prepared from $\text{Cd}(\text{Ac})_2$ became turbid after cooling due to the poor solubility of unreacted cadmium acetate in the HDA–TOPO–TOP mixture. In this case the solutions were filtrated before measurements through a $0.2\text{-}\mu\text{m}$ PTFE syringe filter.

CdSe nanocrystals synthesized from dimethylcadmium displayed a very high reaction yield at early stages of the synthesis. After several minutes of the heating, approximately 80% of Se precursor was converted into CdSe nanocrystals and the reaction yield slightly increased up to $>90\%$ upon further heating (Figure 2). A different behavior was observed when $\text{Cd}(\text{Ac})_2$ was used as a Cd precursor. After nucleation only $\sim 20\%$ of cadmium acetate was converted to CdSe nanocrystals and the particle growth was accompanied by considerable increase of the reaction yield (Figure 2). After prolonged heating the reaction yield approached $\sim 90\%$ and stayed at this level during further growth.

The huge difference in particle growth rate and the temporal evolution of the reaction yield can be understood if we suggest different regimes of nanocrystal growth for different Cd precursors. Thus, $\text{Cd}(\text{CH}_3)_2$ is extremely reactive and decomposes immediately after injecting into the hot reaction mixture.^{12,40} In presence of TOPSe, all cadmium precursors will promptly convert into CdSe nanocrystals at an early stage of the process. Further growth can only occur via Ostwald ripening, i.e., the larger particles within an ensemble grow at the expense

of the smaller ones.⁴¹ The increase of the particle size is accompanied by a decrease in the particle concentration and the reaction yield remains high at all stages of synthesis. Recently, we have found that Ostwald ripening of nanosized particles differs markedly from that of larger particles. Thus, nano-Ostwald ripening is considerably faster and results in narrower size distributions.⁴² On the other hand, $\text{Cd}(\text{Ac})_2$ is relatively stable and can survive in the HDA–TOPO–TOP mixture at $260\text{--}300$ °C for a long period of time. Injection at 300 °C results in nucleation of CdSe particles. The subsequent drop of the temperature quenches the nucleation of new particles, even though most of the cadmium acetate is still unreacted. The nucleated nanocrystals in this case will grow, consuming molecular precursors from the surrounding solution. Nanocrystal growth in this regime is accompanied by narrowing the size distribution and is, therefore, called the “focusing growth regime”.⁴² The particle concentration remains nearly constant and the reaction yield should increase with increase of nanocrystal size (Figure 2). When nearly all molecular precursors are consumed, further nanocrystal growth is governed by nano-Ostwald ripening.

Reaction Yield and One-Pot Preparation of Core–Shell Nanocrystals. Information about the reaction yield is very important for one-pot synthesis of core–shell nanocrystals. Indeed, the current concentration of core nanocrystals is required to estimate the amount of shell precursors necessary for a desired shell thickness. If $\text{Cd}(\text{CH}_3)_2$ is used as the Cd precursor, CdSe nanocrystals form with almost 100% reaction yield at all stages of the synthesis. This means that the crude solution does not contain large amounts of the molecular precursors taken for the synthesis of CdSe core nanocrystals. Introducing the shell precursors allows the formation of nanoparticles with a distinct core–shell structure, as was successfully realized, e.g., in the synthesis of CdSe/ZnS nanocrystals.^{13,28} Synthesis of CdSe nanocrystals from cadmium acetate usually occurs with the reaction yields far below 100%, especially for particles smaller than ~ 4 nm (Figure 2). This means that the crude solution contains an excess of Cd and Se precursors, and one-pot synthesis of core–shell particles is possible only if the shell precursors have much higher reactivity than the core precursors. Probably, this behavior is typical also for other “greener” cadmium precursors.

Synthesis of CdSe/CdS Core–Shell Nanocrystals. The synthesis of luminescent CdSe/CdS core–shell particles in the TOPO–TOP reaction mixture was unsuccessful.³⁰ Addition of cadmium and sulfur precursors into the solution of CdSe nanocrystals resulted in homogeneous nucleation of new CdS particles rather than formation of CdS shells around CdSe nanocrystals. Probably, the barrier for nucleation of CdS nanocrystals is too low in the TOPO–TOP mixture. It was then decided to attempt the CdS shell growth in the HDA–TOPO–TOP mixture. This mixture was chosen because the HDA–TOP mixture was found to be suitable for the synthesis of monodisperse CdS nanocrystals,³³ which seems to be a good hint to expect controllable growth of a CdS shell in the presence of HDA and TOP stabilizing agents. Moreover, the HDA–TOPO–TOP mixture provides outstanding conditions for synthesis of monodisperse CdSe nanocrystals, which can be further used as cores without size-selective fractionation.¹³

We have found that slow addition of H_2S gas to the crude solution of CdSe nanocrystals prepared from $\text{Cd}(\text{Ac})_2$ results in a drastic improvement of PL efficiency of the colloidal solution. The temperature of the crude solution was adjusted to 140 °C before the injection of H_2S . For the sample shown in

Figure 3 the addition of H_2S gas resulted in improving PL QE from 28% up to 85%. Similar improvement of the PL properties was observed for all samples with different initial size of CdSe nanocrystals.

The progressive injection of H_2S gas produced red shifts of both the first absorption maximum and the PL band (Figure 3). The maximum red shift was larger (up to 33 nm) if the injection of H_2S gas was performed into a crude solution of small (~ 3 nm) CdSe nanocrystals, whereas the same procedure performed for the crude solutions of larger (~ 5 nm) CdSe nanocrystals resulted in considerably smaller red shifts (~ 6 – 12 nm). The XRD pattern of highly luminescent nanocrystals prepared as described above has roughly the same shape as that of pure CdSe cores; however, the diffraction angles are shifted to larger 2θ values and lie between those inherent to CdSe and CdS wurtzite phases (Figure 4). Such an XRD pattern can correspond to either $\text{CdS}_x\text{Se}_{1-x}$ alloy or CdSe/CdS core-shell nanocrystals.³⁰ On the other hand, the formation of $\text{CdS}_x\text{Se}_{1-x}$ alloy nanocrystals, e.g., via substitution of selenium surface atoms with sulfur, would result in a blue shift of absorption and PL spectra because of the larger band gap energy of $\text{CdS}_x\text{Se}_{1-x}$ compared to pure CdSe.⁴⁴ The observed red shifts are therefore understood as a strong indication for the formation of a CdSe/CdS core-shell structure.

TEM investigations show that the injection of H_2S gas results in an increase in nanocrystal size (Figure 5). The lattice fringes stretch through the entire nanocrystals, indicating that the increase in the particle size does not disturb their crystallinity. The increase of the nanocrystal size was more pronounced for small nanocrystals, whereas in the case of ~ 4.8 -nm CdSe nanocrystals the improvement of PL QE is already achieved with a minor increase of the average particle size (Figure 5). EDAX measurements clearly show the presence of cadmium, selenium, and sulfur in thoroughly washed highly luminescent nanocrystals.

Summarizing, we have strong evidence that injection of H_2S into crude solutions of CdSe nanocrystals in the HDA-TOPO-TOPO mixture results in growth of an outer CdS shell around CdSe cores. We can, however, not rule out that the outer shell consists of $\text{CdS}_x\text{Se}_{1-x}$ alloy or exhibits a gradient composition. As discussed above, the reaction yield is relatively low, especially for small CdSe nanocrystals, if $\text{Cd}(\text{Ac})_2$ is used as a precursor (Figure 2), and a considerable amount of unreacted cadmium precursor is present in the crude solution after formation of CdSe cores. Probably, the H_2S gas has a much higher reactivity with respect to cadmium acetate in comparison to TOPSe. Note, that the latter is present in the reaction mixture in large excess. However, no growth of CdSe nanocrystals was observed at 140°C in control experiments. In contrast, at this temperature H_2S immediately reacts with $\text{Cd}(\text{Ac})_2$, yielding CdS. The presence of HDA in the stabilizing mixture promotes absorption of H_2S gas due to formation of highly reactive hexadecylammonium sulfide. In fact, nucleation of individual CdS nanocrystals was also observed in some experiments; however, optimizing the experimental conditions (proper temperature control, stepwise addition of H_2S above the solution) allowed us to suppress the nucleation of new CdS nanocrystals. The EDAX measurements performed on the samples with different shell thickness show that the content of selenium in the shell is low. Unfortunately, the analysis of exact shell composition is very difficult. Thus, in the case of CdSe/ZnS core-shell nanocrystals, the depth profiles for sulfur and selenium could not be estimated by the high-resolution XPS due to the overlap of S 2p and Se 3p core levels.⁴⁵

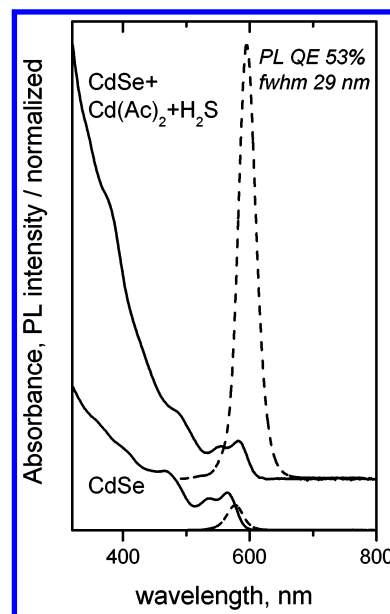


Figure 6. Absorption (solid) and PL (dashed) spectra of CdSe nanocrystals synthesized from dimethylcadmium and TOPSe and CdSe/CdS core-shell nanocrystals prepared from these CdSe cores by adding cadmium acetate and H_2S at 140°C .

Thus, the reported method allows a simple and routine preparation of highly luminescent nanocrystals emitting with room-temperature PL QE of 50–85% from green to red, depending on the initial size of CdSe nanocrystals. Moreover, these nanocrystals can be prepared in relatively large amounts, as no diluting of the CdSe crude solution is necessary before the injection of H_2S gas. No expensive or dangerous organometallic reagents were used in synthesis of both CdSe core and CdS shell.

Tuning Thickness of CdS Shell in One-Pot Synthesis of CdSe/CdS Nanocrystals. Both PL QE and stability of the luminescent properties of core-shell nanocrystals strongly depend on the thickness of the inorganic passivating shell.^{29,30} The control of the CdS shell thickness is therefore of great importance for the preparation of CdSe/CdS nanocrystals with predictable and stable luminescent properties. However, the synthesis of CdSe/CdS nanocrystals with predictable thickness of CdS shell via the method described above is somewhat difficult. Indeed, the amount of the formed CdS phase is reverse proportional to the reaction yield. The reaction yield is a parameter which depends on the nanocrystal size, varies from run to run, and is too complex to be precisely controlled.

To obtain a CdS shell of a desired thickness around CdSe cores, one can synthesize CdSe from $\text{Cd}(\text{CH}_3)_2$ and TOPSe. In this case a nearly quantitative reaction yield was observed at all stages of CdSe nanocrystal growth (Figure 2) and a current concentration of CdSe nanocrystals can be calculated from the initial amounts of precursors and the current particle size. The latter can easily be estimated from the spectral position of the first absorption maximum.³⁸ Injection of H_2S gas into the crude solution of organometallically prepared CdSe nanocrystals did not result in improvement of the PL QE. However, if $\text{Cd}(\text{Ac})_2$ was added to the crude solution of CdSe nanocrystals, the injection of H_2S gas resulted in drastic improvement of the PL QE and caused red shifts of both UV-vis and PL spectra (Figure 6). By varying the amount of added cadmium acetate we were able to tune the thickness of the CdS shell around CdSe nanocrystals. Note that in this case the crude solution of CdSe nanocrystals did not contain excess Se precursor, a condition which seems to favor the growth of a pure CdS shell.

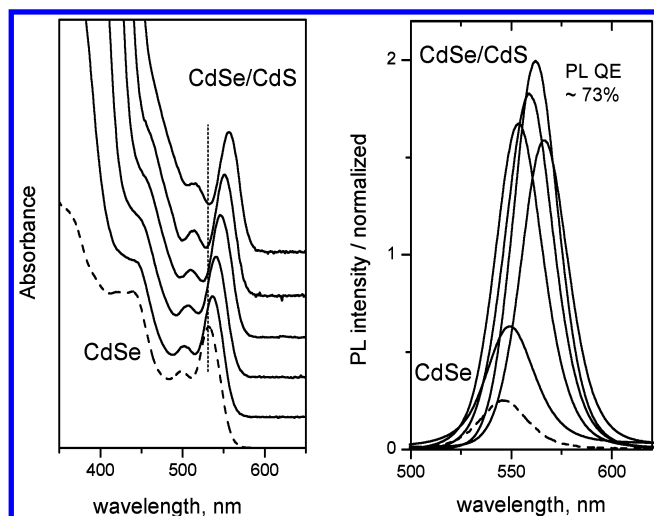


Figure 7. Evolution of absorption (left) and PL (right) spectra with increasing thickness of CdS shell around CdSe nanocrystals. Progressive red shift of the first absorption maximum and PL band accompanies the increase of CdS shell thickness from 0 up to ~ 3.5 monolayers. The CdSe cores (dashed spectra) were synthesized from dimethylcadmium + TOPSe and the CdS shell was grown by a stepwise addition of the dimethylcadmium and bistrimethylsilylsulfide stock solution at 140 °C.

CdS shells with adjustable thickness can also be synthesized in HDA–TOPO–TOP mixtures from organometallic precursors. Thus, we used a crude solution of ~ 3.5 -nm CdSe nanocrystals prepared from $\text{Cd}(\text{CH}_3)_2$ and added a solution of cadmium and sulfur precursors, i.e., $\text{Cd}(\text{CH}_3)_2$ and $((\text{CH}_3)_3\text{Si})_2\text{S}$ dissolved in TOP (see the Experimental Section). Dropwise addition of the shell precursors at 140–150 °C resulted in controllable growth of a CdS shell around the CdSe cores (Figure 7). Using an excess of sulfur precursor with respect to cadmium precursor (molar ratio $\sim 1.5:1$ – $2:1$) suppresses the homogeneous nucleation of CdS nanocrystals completely and yields pure colloidal solutions of CdSe/CdS nanocrystals without post-preparative fractionation of core–shells from nucleated CdS nanocrystals. In this case the amount of Cd:S precursors necessary to obtain the desired shell thickness can be calculated from the ratio between the core and shell volumes by using bulk lattice parameters of CdSe and CdS. The observed red shifts upon increasing the thickness of the CdS shell can be explained by spreading the electrons over the entire nanocrystal, while the hole remains confined in the CdSe core.³⁰ Surprisingly, the nanocrystal size distribution keeps exceptionally narrow during all stages of shell growth in the HDA–TOPO–TOP mixture, as is evidenced from well-resolved sharp transitions in UV–vis spectrum, the narrow PL bands (Figure 7), and the TEM investigations (Figures 5 and 8).

Stability of PL Properties under UV Illumination for CdSe, CdSe/CdS, and CdSe/ZnS Nanocrystals. The surface structure and surface environment are the parameters mainly affecting the PL QE of semiconductor nanocrystals.^{23,45} Recent studies have shown that the PL QE does not seem to be very sensitive to the imperfection of the crystallinity of the nanocrystals caused by stacking faults,^{23,47} whereas the “correct” surface reconstruction^{23,38} or adsorption of some organic ligands (e.g., primary amines)^{13,48} can improve the nanocrystal PL QE dramatically. On the other hand, partial removing of the stabilizing agents can result in a decrease of band-edge luminescence by orders of magnitude.⁴⁷ Due to sensitivity of the nanocrystal luminescence to all processes occurring at the particle surface, the stability of the PL properties becomes a

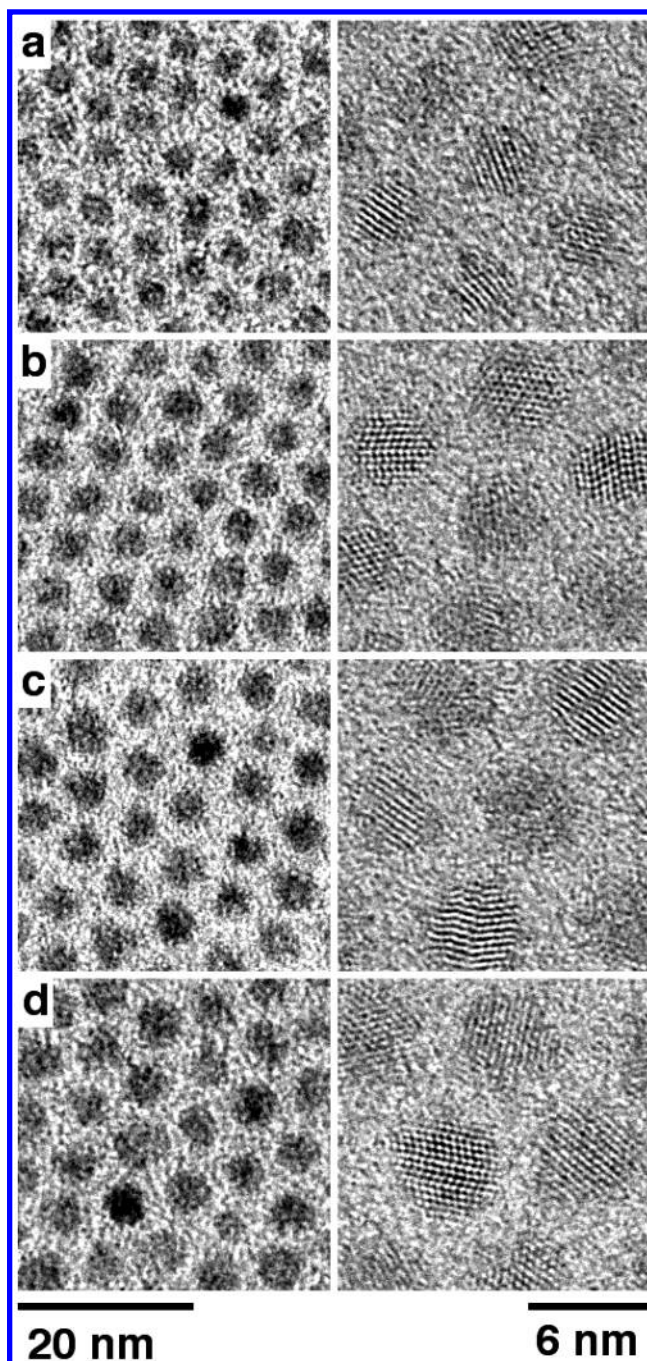


Figure 8. Overview TEM (left) and HRTEM (right) images of as-prepared (a) CdSe nanocrystal cores and (b, c, d) CdSe/CdS core–shell particles with gradually increased thickness of the CdS shell. Absorption spectra and powder XRD patterns of all samples are shown in the supporting information.

very important parameter for applying luminescent nanocrystals in optoelectronic devices or luminescent labels.

The “bare” colloidal nanocrystals are capped with a shell of organic ligands (TOPO, TOP, HDA) which provide an effective electronic passivation of surface dangling bonds. However, a bottleneck of the organic ligands is their relatively poor chemical stability and weak binding to the nanocrystal surface. For instance, amines are well-known as sacrificial donors (hole scavengers) in photocatalysis. This behavior causes instability of the nanocrystal properties under UV illumination. On the other hand, the passivation of the nanocrystal surface with an inorganic shell increases the stability of the PL QE considerably.^{29,30} Indeed, most of the CdSe/CdS nanocrystal samples

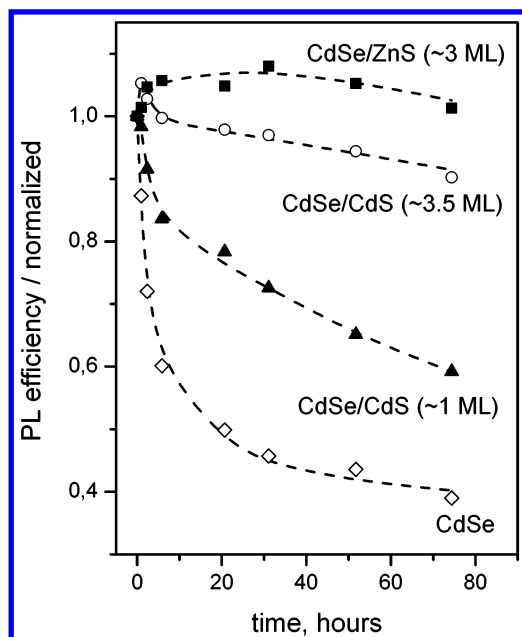


Figure 9. Stability of the PL quantum efficiency of the HDA–TOPO–TOP capped CdSe, CdSe/CdS, and CdSe/ZnS nanocrystals under illumination with UV light (366 nm). For the core–shell nanocrystals the thickness of the shell in monolayers (ML) is shown. The PL efficiency of each sample was normalized to its initial value observed before the illumination. The initial PL quantum efficiency was 52% for CdSe; 48% for CdSe/CdS with ~1 monolayer thick CdS shell; 58% for CdSe/CdS with ~3.5 monolayer thick CdS shell, and 42% for CdSe/ZnS core–shell nanocrystals.

prepared in framework of this study retain their PL properties for almost a year under air and daylight.

To further investigate the stability of PL properties and test the quality of CdS shell formed around CdSe nanocrystals, we have performed a comparative study of the stability of the PL QE of CdSe and CdSe/CdS nanocrystals under UV irradiation (366 nm). Note that all nanocrystal samples, CdSe, CdSe/CdS, and CdS/ZnS, were capped with the HDA–TOPO–TOP ligand shell, allowing us to compare the nanocrystal properties rather than the stability of various organic ligands. Moreover, we compared the photostability of our CdSe/CdS nanocrystals with that of CdSe/ZnS core–shells, which are, probably, the most stable luminescent nanocrystals known to date. Figure 9 shows the evolution of the PL QE vs illumination time for CdSe, CdSe/ZnS, and two samples of CdSe/CdS nanocrystals with different thickness of CdS shell (~1 and 3.5 monolayers). Bare CdSe nanocrystals capped with organic ligands retained half of their initial quantum efficiency after ~20 h of illumination (Figure 9). The losses of quantum efficiency were not accompanied by any changes in the absorption spectrum of nanocrystal solution. No blue shift for the first absorption maximum was observed. This means that no changes the nanocrystal size occurred during the illumination and the decrease of PL QE is related to some processes at the nanocrystal surface. Probably, the photogenerated carriers (presumably holes) captured by the nanocrystal surface states may cause structural changes at the surface of CdSe nanocrystals or promote photocatalytic degradation of the organic capping ligands.²⁷ However, even a thin (~1 monolayer) shell of CdS around CdSe nanocrystals considerably improved stability of the PL QE under UV illumination (Figure 9). In the CdSe/CdS core–shell nanocrystals the holes are confined to the CdSe core and their interaction with the nanocrystal surface is hindered.³⁰ Increasing thickness of the CdS shell up to ~3.5 monolayers resulted in further improvement of the luminescence stability. Thus, the CdSe/CdS nanocrystals re-

tained ~90% of their initial PL QE even after 80 h of UV illumination (Figure 9).

The CdSe/ZnS core–shell nanocrystals exhibit the best stability of PL QE (Figure 9). Their PL efficiency even improved at the beginning of illumination, probably due to photochemical annealing of the structural defects initially presenting at the CdSe–ZnS interface.⁴⁹ Difference in the stability of CdSe/ZnS and CdSe/CdS nanocrystals might originate from the fact that the ZnS shell could not directly be excited by the 366-nm light, whereas the CdS shell absorbs light and may undergo slow photodegradation. Other explanations may involve the different band offsets of both systems leading to a stronger localization of electron and hole in the CdSe core in the case of ZnS shell or different redox potentials for hole traps in the respective shell materials.

An extremely high stability of the luminescence of CdSe/CdS core–shell nanocrystals was also observed during formation of CdSe/CdS composites with poly(lauryl methacrylate) (PLMA) matrix prepared by radical polymerization of lauryl methacrylate in the presence of luminescent nanocrystals according to the recipe proposed in ref 33.

Conclusions

A comparative study of the organometallic and “greener” synthesis of CdSe nanocrystals in the HDA–TOPO–TOP mixture revealed a general difference between these approaches. In the organometallic scheme, the highly reactive dimethylcadmium promptly converts to the CdSe nanocrystals which grow via the nano-Ostwald ripening mechanism.⁴² In contrast, “greener” cadmium precursors (e.g., cadmium acetate) are considerably more stable in the HDA–TOPO–TOP mixture, and only ~20% of cadmium precursor converts to the CdSe nanocrystals during the nucleation stage. The nanocrystals presumably grow in the focusing regime,⁴³ consuming free monomers from surrounding solution and a high amount of free molecular precursors is still present in the crude solution of CdSe nanocrystals. This fact must be taken into account if these CdSe cores are used in a one-pot synthesis of core–shell nanocrystals. Thus, injecting H₂S gas at 140 °C into the crude solution containing both CdSe nanocrystals and unreacted cadmium acetate results in formation of epitaxial CdS shells around CdSe cores. Moreover, the HDA–TOPO–TOP mixture was found to be nearly ideal for controllable growth of monodisperse CdSe/CdS nanocrystals with the room-temperature PL quantum efficiency as high as 50–85%. The stability of the PL efficiency of so-prepared CdSe/CdS nanocrystals is considerably higher under UV illumination than that of bare CdSe nanocrystals. The CdSe/CdS particles with a ~3.5 monolayer thick CdS shell were almost as stable as the CdSe/ZnS particles.

The proposed method of one-pot synthesis CdSe/CdS nanocrystals in the HDA–TOPO–TOP mixture can, probably, be extended to a one-pot preparation of a more complex structure where the CdSe core is consecutively capped with CdS and ZnS shells. Potentially, these core/shell/shell nanoparticles allow combining very high PL quantum efficiency inherent to CdSe/CdS nanocrystals with the stability of CdSe/ZnS nanocrystals. This study is currently under way.

Acknowledgment. We thank Sylvia Bartholdi-Nawrath for assistance with TEM and HRTEM investigations. This work was supported by the BMBF, Philips, and by the Deutsche Forschungsgemeinschaft through the SFB 508.

Supporting Information Available: Absorption spectra and powder XRD patterns of CdSe and CdSe/CdS nanocrystal

samples shown in Figure 8. This material is available free of charge via the Internet at <http://pubs.acs.org>.

References and Notes

- (1) Gaponenko, S. V. *Optical Properties of Semiconductor Nanocrystals*; Cambridge University Press: Cambridge, UK, 1998.
- (2) Woggon, U. *Optical Properties of Semiconductor Quantum Dots*; Springer-Verlag: Berlin, Germany, 1997.
- (3) Alivisatos, A. P. *J. Phys. Chem.* **1996**, *100*, 13226.
- (4) Colvin, V. L.; Schlamp, M. C.; Alivisatos, A. P. *Nature* **1994**, *370*, 354.
- (5) Tessler, N.; Medvedev, V.; Kazes, M.; Kan, S. H.; Banin, U. *Science* **2002**, *295*, 1506.
- (6) Klimov, V. I.; Mikhailovsky, A. A.; Xu, S.; Hollingsworth, J. A.; Leatherdale, C. A.; Eisler, H. J.; Bawendi, M. G. *Science* **2000**, *290*, 314.
- (7) Harrison, M. T.; Kershaw, S. V.; Burt, M. G.; Rogach, A. L.; Kornowski, A.; Eychmüller, A.; Weller, H. *Pure Appl. Chem.* **2000**, *72*, 295.
- (8) Bruchez, M. P.; Moronne, M.; Gin, P.; Weiss, S.; Alivisatos, A. P. *Science* **1998**, *281*, 2013.
- (9) Dubertret, B.; Skourides, P.; Norris, D. J.; Noireaux, V.; Brivanlou, A. H.; Libchaber, A. *Science* **2002**, *298*, 1759.
- (10) Murray, C. B.; Kagan, C. R.; Bawendi, M. G. *Science* **1995**, *270*, 1335.
- (11) Rogach, A. L.; Talapin, D. V.; Shevchenko, E. V.; Kornowski, A.; Haase, M.; Weller, H. *Adv. Funct. Mater.* **2002**, *12*, 653.
- (12) Murray, C. B.; Norris, D. J.; Bawendi, M. G. *J. Am. Chem. Soc.* **1993**, *115*, 8706.
- (13) Talapin, D. V.; Rogach, A. L.; Kornowski, A.; Haase, M.; Weller, H. *Nano Lett.* **2001**, *1*, 207.
- (14) Gaponik, N.; Talapin, D. V.; Rogach, A. L.; Hoppe, K.; Shevchenko, E. V.; Kornowski, A.; Eychmüller, A.; Weller, H. *J. Phys. Chem. B* **2002**, *106*, 7177.
- (15) Yu, W. W.; Peng, X. *Angew. Chem., Int. Ed. Engl.* **2002**, *41*, 2368.
- (16) Peng, X.; Manna, L.; Yang, W. D.; Wickham, J.; Scher, E.; Kadavanich, A.; Alivisatos, A. P. *Nature* **2000**, *404*, 59.
- (17) Micic, O. L.; Curtis, C. J.; Jones, K. M.; Sprague, J. R.; Nozik, A. J. *J. Phys. Chem.* **1994**, *98*, 4966.
- (18) Guzelian, A. A.; Banin, U.; Kadavanich, A. V.; Peng, X.; Alivisatos, A. P. *Appl. Phys. Lett.* **1996**, *69*, 1432.
- (19) Talapin, D. V.; Gaponik, N.; Borchert, H.; Rogach, A. L.; Haase, M.; Weller, H. *J. Phys. Chem. B* **2002**, *106*, 12659.
- (20) Cao, Y. W.; Banin, U. *J. Am. Chem. Soc.* **2000**, *122*, 9692.
- (21) Manna, L.; Scher, E. C.; Alivisatos, A. P. *J. Am. Chem. Soc.* **2000**, *122*, 12700.
- (22) Peng, X. *Chem. Eur. J.* **2002**, *8*, 335.
- (23) Qu, L.; Peng, X. *J. Am. Chem. Soc.* **2002**, *124*, 2049.
- (24) Peng, Z. A.; Peng, X. *J. Am. Chem. Soc.* **2001**, *123*, 183.
- (25) Peng, Z. A.; Peng, X. *J. Am. Chem. Soc.* **2002**, *124*, 3343.
- (26) Qu, L.; Peng, Z. A.; Peng, X. *Nano Lett.* **2001**, *1*, 333.
- (27) Aldana, J.; Wang, Y. A.; Peng, X. *J. Am. Chem. Soc.* **2001**, *123*, 8844.
- (28) Hines, M. A.; Guyot-Sionnest, P. *J. Phys. Chem.* **1996**, *100*, 468.
- (29) Dabbousi, B. O.; Rodriguez-Viejo, J.; Mikulec, F. V.; Heine, J. R.; Mattoussi, H.; Ober, R.; Jensen, K. F.; Bawendi, M. *J. Phys. Chem. B* **1997**, *101*, 9463.
- (30) Peng, X.; Schlamp, M. C.; Kadavanich, A.; Alivisatos, A. P. *J. Am. Chem. Soc.* **1997**, *119*, 7019.
- (31) Reiss, P.; Bleuse, J.; Pron, A. *Nano Lett.* **2002**, *2*, 781.
- (32) Ebenstein, Y.; Mokari, T.; Banin, U. *Appl. Phys. Lett.* **2002**, *80*, 4033.
- (33) Lee, J.; Sundar, V. C.; Heine, J. R.; Bawendi, M. G.; Jensen, K. F. *Adv. Mater.* **2000**, *12*, 1102.
- (34) Gerion, D.; Pinaud, F.; Williams, S. C.; Parak, W. J.; Zanchet, D.; Weiss, S.; Alivisatos, A. P. *J. Phys. Chem. B* **2001**, *105*, 8861.
- (35) Schlamp, M. C.; Peng, X.; Alivisatos, A. P. *J. Appl. Phys.* **1997**, *82*, 5837.
- (36) de Mello Donega, C.; Hickey, S. G.; Wuister, S. F.; Vanmaekelbergh, D.; Meijerink, A. *J. Phys. Chem. B* **2003**, *107*, 489.
- (37) Kubin, R. F.; Fletcher, A. N. *J. Lumin.* **1982**, *27*, 455.
- (38) Sizes and size distributions were estimated from the absorption and PL spectra as described in ref 43 using sizing curves for CdSe quantum dots from the Supporting Information to the paper by: Mikulec, F. V.; Kuno, M.; Bennati, M.; Hall, D. A.; Griffin, R. G.; Bawendi, M. G. *J. Am. Chem. Soc.* **2000**, *122*, 2532.
- (39) Schmelz, O.; Mews, A.; Basché, T.; Herrman, A.; Müllen, K. *Langmuir* **2001**, *17*, 2861.
- (40) Leatherdale, C. A.; Woo, W.-K.; Mikulec, F. V.; Bawendi, M. G. *J. Phys. Chem. B* **2002**, *106*, 7619.
- (41) Talapin, D. V.; Rogach, A. L.; Shevchenko, E. V.; Kornowski, A.; Haase, M.; Weller, H. *J. Am. Chem. Soc.* **2002**, *124*, 5782.
- (42) Talapin, D. V.; Rogach, A. L.; Haase, M.; Weller, H. *J. Phys. Chem. B* **2001**, *105*, 12278.
- (43) Peng, X.; Wickham, J.; Alivisatos, A. P. *J. Am. Chem. Soc.* **1998**, *120*, 5343.
- (44) Streckert, H. H.; Ellis, A. B. *J. Phys. Chem.* **1982**, *86*, 4921.
- (45) Borchert, H.; Talapin, D. V.; McGinley, C.; Adam, S.; de Castro, A. R. B.; Möller, T.; Weller, H. *J. Chem. Phys.*, in press.
- (46) Potapova, I.; Mruk, R.; Prehl, S.; Zentel, R.; Basché, T.; Mews, A. *J. Am. Chem. Soc.* **2003**, *125*, 320.
- (47) Koberling, F.; Mews, A.; Philipp, G.; Kilb, U.; Potapova, I.; Burghard, M.; Basché, T. *Appl. Phys. Lett.* **2002**, *81*, 1116.
- (48) Talapin, D. V.; Rogach, A. L.; Mekis, I.; Haubold, S.; Kornowski, A.; Haase, M.; Weller, H. *Colloids Surf. A* **2002**, *202*, 145.
- (49) Manna, L.; Scher, E. C.; Li, L.-S.; Alivisatos, A. P. *J. Am. Chem. Soc.* **2002**, *124*, 7136.